Articles
doi.org/10.1002/batt.201900197

Chemistry Europe
European Chemical Societies Publishing

Special Collection

Effects of Anion on Liquid Structures of Ionic Liquids at Graphene Electrode Interface Analyzed by Molecular Dynamics Simulations

Seiji Tsuzuki,*[a] Takenobu Nakamura,[a] Tetsuya Morishita,[a] Wataru Shinoda,[b] Shiro Seki,[c] Yasuhiro Umebayashi,[d] Kazuhide Ueno,[e] Kaoru Dokko,[e, f] and Masayoshi Watanabe[e]

Molecular dynamics simulations of ionic liquids composed of *N*-propyl-*N*-methylpyrrolidinium cation ([pmpyro]$^+$) with $(CF_3SO_2)_2N^-$ ([TFSA]$^-$), $(FSO_2)_2N^-$ ([FSA]$^-$), $CF_3SO_3^-$, $CF_3CO_2^-$ and PF_6^- anions sandwiched by two charged graphene sheets show that the liquid structures near graphene sheets depend strongly on anion. Long-range charge ordering structures were observed when the ionic liquids were sandwiched with charged graphene sheets. Although the magnitude of the oscillation of cation and anion densities near charged graphene sheets is enhanced by the increase of the charges on the graphene sheets, the range of the charge-ordering structures from the graphene sheets does not largely change. The ranges of the charge-ordering structures from charged graphene sheets observed in the [pmpyro][TFSA], [pmpyro][FSA], [pmpyro][CF_3SO_3], [pmpyro][CF_3CO_2] and [pmpyro][PF_6] ionic liquids are approximately 40, 80, 60, 60 and 100 Å, respectively.

1. Introduction

Ionic liquids attract considerable interest as candidates of electrolytes for electronic devices such as lithium ion batteries and capacitors, owing to the negligible vapor pressure, low flammability, high ionic conductivity and electrochemical stability of ionic liquids.[1–4] The liquid structure of the ionic liquid at the electrode interface is important for the performance of the electronic devices and detailed information on the liquid structure at the interface is essential for understanding reactions at the electrode. For this reason, the liquid structures of ionic liquids at the electrode interface were studied actively by several experimental methods such as surface-enhanced infrared absorption spectroscopy (SEIRAS),[5–8] sum frequency generation spectroscopy (SFG),[9–11] and atomic ***force microscopy*** (AFM).[12–17] The measurements by SEIRAS and SFG provide information on the orientation of ions in ionic liquids near the interface. The AFM measurements shows the existence of layer structures near the interface. Although various valuable information on the liquid structure of the ionic liquid at the electrode interface have been obtained from these experimental measurements, it is still not easy to elucidate the details of the liquid structure (distribution and orientation of each ion) at the electrode interface only by experimental methods.

The liquid structures of ionic liquids at the electrode interfaces were also studied by molecular dynamics (MD) simulations.[18–34] MD simulations can provide detailed information on the liquid structures at the molecular level. Pyrrolidinium cation-based ionic liquids are often used for electrolytes for batteries. The battery performance depends on the choice of the cation and anion of the ionic liquid used for the electrolyte. A few MD simulations of pyrrolidinium-based ionic liquids were reported.[23,27,30–34] The effects of chain length and branching of alkyl groups of pyrrolidinium cations on the liquid structures at the interface have been studied by MD simulations.[33,34] On the other hand, the effects of anions on the liquid structures of the ionic liquids at the electrode interface were not well understood. Therefore, we carried out MD simulations of ionic liquids composed of *N*-propyl-*N*-methylpyrrolidinium cation ([pmpyro]$^+$) and several anions [$(CF_3SO_2)_2N^-$ ([TFSA]$^-$), $(FSO_2)_2N^-$ ([FSA]$^-$), $CF_3SO_3^-$, $CF_3CO_2^-$ and PF_6^-] to elucidate the effects of the choice of anion on the liquid structures at the electrode interface.

[a] *Dr. S. Tsuzuki, Dr. T. Nakamura, Dr. T. Morishita*
Research Center for Computational Design of Advanced Functional Materials (CD-FMat)
National Institute of Advanced Industrial Science and Technology (AIST)
1-1-1 Umezono, Tsukuba, Ibaraki 305-8568, Japan
Fax: (+81) 29 851 5426
E-mail: s.tsuzuki@aist.go.jp
[b] *Prof. W. Shinoda*
Department of Materials Chemistry, Nagoya University
Furo-cho, Chikusa-ku, Nagoya 464-8603, Japan
[c] *Prof. S. Seki*
Department of Environmental Chemistry and Chemical Engineering
School of Advanced Engineering, Kogakuin University
2665-1 Nakano-machi, Hachioji, Tokyo 192-0015, Japan
[d] *Prof. Y. Umebayashi*
Graduate School of Science and Technology Niigata University 8050
Ikarashi, 2-no-cho, Nishi-ku, Niigata 950-2181, Japan
[e] *Prof. K. Ueno, Prof. K. Dokko, Prof. M. Watanabe*
Department of Chemistry and Biotechnology, Yokohama National University
79-5 Tokiwadai, Hodogaya-ku, Yokohama 240-8501, Japan
[f] *Prof. K. Dokko*
Unit of Elements Strategy Initiative for Catalysts & Batteries (ESICB)
Kyoto University, Kyoto 615-8510, Japan

Supporting information for this article is available on the WWW under https://doi.org/10.1002/batt.201900197

Special Collection *An invited contribution to a Special Collection on Electrolytes for Electrochemical Energy Storage*

Computational Methods

Molecular dynamics simulations of ionic liquids sandwiched with charged graphene sheets (Figure 1) were carried out. LAMMPS (7Dec2015) program[34] was used for the molecular dynamics simulations. Each graphene sheet (22.050×21.218 Å) was consisted with 180 carbon atoms. The numbers of ion pairs used for the simulations are 165–233. The distances between two graphene sheets are about 200 Å. The thickness of vacuum layer is 100 Å. Numbers of ion pairs and the distances between two graphene sheets in the simulations are summarized in Table S1 in supporting information. All the C–H bonds were held rigid using the SHAKE algorithm.[35] The time step size was 2 fs. Periodic boundary conditions were employed. The nonbonded forces were truncated at 10 Å. Constant-temperature was maintained by using the Nose-Hoover chain thermostat.[36] The force field used for the simulations are shown in elsewhere.[37] After a 1 ns equilibration run, a 40 ns production run was made at 603 K to calculate the density of ions.

The densities of ionic liquids between graphene sheets are identical to the densities of bulk ionic liquids obtained by constant pressure molecular dynamics simulations at the same temperature. The density of center of mass of cations and anions were calculated to discuss the liquid structure of ionic liquids between graphene sheets. The cation and anion densities shown in Figures were normalized by the average densities of ions in bulk ionic liquids.

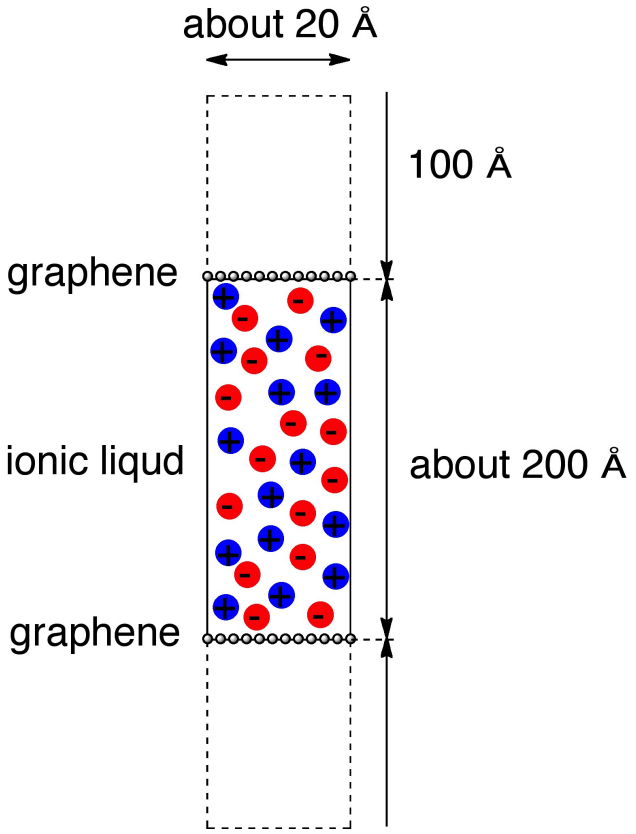

Figure 1. Unit cell used for molecular dynamic simulations. Number of ion pairs and distance between graphene sheets are shown in Table S1.

2. Results and Discussion

2.1. Charge Distributions of [pmpyro]$^+$ Cation and [TFSA]$^-$ Anion

The electrostatic potentials calculated for [pmpyro]$^+$ cation and [TFSA]$^-$ anion are shown in Figure 2. Positively charged region is shown in red and negatively charged region is shown in blue. Positive charges of [pmpyro]$^+$ cation mainly distribute not only on the nitrogen atom but also on methyl and methylene groups connected with the nitrogen atom. The positive charges on other methyl and methylene groups are small. Negative charges of [TFSA]$^-$ anion mainly distribute on the oxygen and nitrogen atoms. The negative charges on fluorine atoms are small. The calculated electrostatic potentials suggest that the charges on the graphene sheets will affect the orientation of [pmpyro]$^+$ cation and [TFSA]$^-$ anion near the charged graphene sheet.

2.2. Ion Density of [pmpyro][TFSA] Ionic Liquid near Charged Graphene

The ionic liquid near the graphene sheets has long-range charge-ordering structure, when the ionic liquid is sandwiched with charged graphene sheets.[19,21,24,25,27–29] Sha et al. reported the reorientation of [pyrolidinium]$^+$ cation in ionic liquids composed of [*N*-alkyl-*N*-methylpyrrolidinium]$^+$ cation and [TFSA]$^-$ anion at charged carbon electrode from molecular dynamics simulations.[33] On the other hand, Motobayashi et al. reported that the reorientation of [pyrolidinium]$^+$ cation was not observed at Au surface from the measurements of SEIRAS.[8]

Ionic liquids near graphene sheet have structures, even if the graphene sheet does not have charges. The normalized ion densities for the [pmpyro][TFSA] ionic liquid sandwiched by graphene sheets without charges obtained by MD simulation are shown in Figure 3a. The calculated ion densities show that the [pmpyro][TFSA] ionic liquid has structure in the range of 20 Å from graphene sheet.

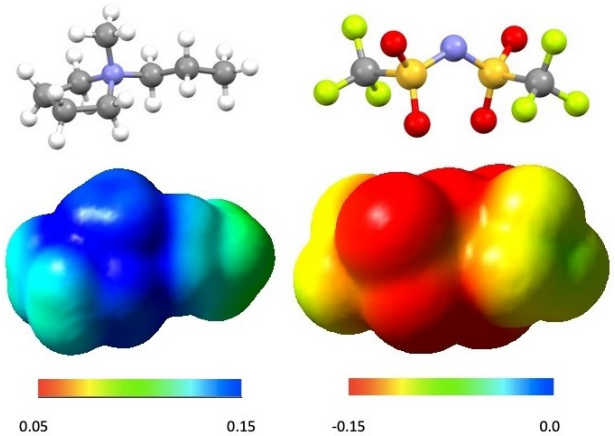

Figure 2. Electrostatic potentials calculated for [pmpyro]$^+$ cation and [TFSA]$^-$ anion in atomic unit.

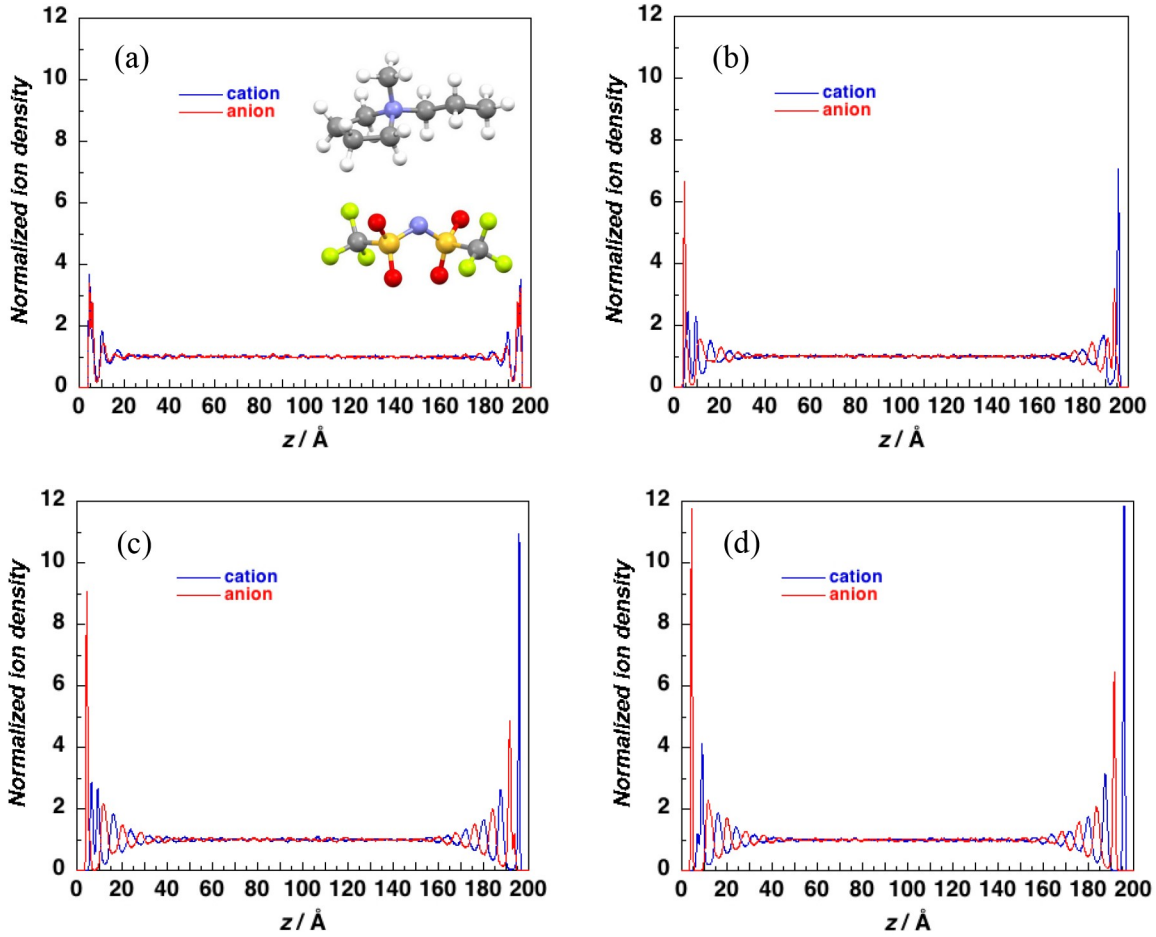

Figure 3. Normalized density of cation and anion obtained by MD simulations of [pmpyro][TFSA] ionic liquid. a) Carbon atoms of graphene have no charges; b) carbon atoms of graphene at $z=0$ Å have 0.01 e and those at $z=200$ Å have −0.01 e; c) carbon atoms of graphene at $z=0$ Å have 0.02 e and those at $z=200$ Å have −0.02 e; d) carbon atoms of graphene at $z=0$ Å have 0.03 e and those at $z=200$ Å have −0.03 e.

The normalized ion densities calculated for the [pmpyro][TFSA] ionic liquid sandwiched by charged graphene sheets are shown in Figures 3b–d. Each carbon atom of the graphene sheet at $z=0$ Å has 0.01 e and that at $z=200$ Å has −0.01 e in the MD simulation of Figure 3b. The charges of carbon atoms in the graphene sheets in the MD simulations in Figure 3c and 3d are ± 0.02 and ± 0.03 e, respectively. In the region closest to graphene, the density of ions having charges opposite to that of graphene sheet increases. In the second closest region, the density of ions with the same charge as graphene increases. In the third closest region, the density of ions having a charge opposite to that of graphene increases again. The magnitude of the ordering of cation and anion decreases slowly with the increase of the distance from the graphene sheet. The charge-ordering structure is observed from graphene down to 40 Å. The increase of the charges on graphene sheets enhances the magnitude of the oscillation of ion densities, while the range of the charge-ordering structure hardly changes by the increase of the charges on graphene sheets.

The calculated ion densities for the [pmpyro][TFSA] ionic liquid suggest there exist cations and anions under two different environments near the graphene sheets. Figure 4a shows the normalized ion densities for the [pmpyro][TFSA] ionic liquid near the graphene sheet when the graphene sheet has no charges. The density of anion has two peaks at $z=4$ and 6 Å, while the density of cation has a peak at $z=4$ Å and a shoulder peak at $z=6$ Å. The existence of the two peaks suggests there exists cations and anions near the graphene sheet under two different environments, respectively. The short distance of center of mass of $[pmpyro]^+$ cation from the graphene sheet shows that the cation peak at $z=4$ Å corresponds to the cations whose pyrrolidinium ring has contact with the graphene and the pyrrolidinium ring is nearly parallel to the graphene. (Figure 5a). The anion peak at $z=4$ Å corresponds to the $[TFSA]^-$ anion whose long axis is nearly parallel to the graphene plane owing to the short distance of the center of mass from the graphene sheet (Figure 5c). The cations and anions for the peaks at $z=6$ Å locate close to the graphene. Although the orientation of the cation and anion when $z=6$ Å is not clear, the propyl group of the cation and the trifluoromethyl group of the anion can have contact with the graphene sheet when $z=6$ Å (Figures 5a and 5c). We call the ions at $z=4$-6 Å as the first layer ions, since they can have contact with the graphene. The peaks of cation and anion

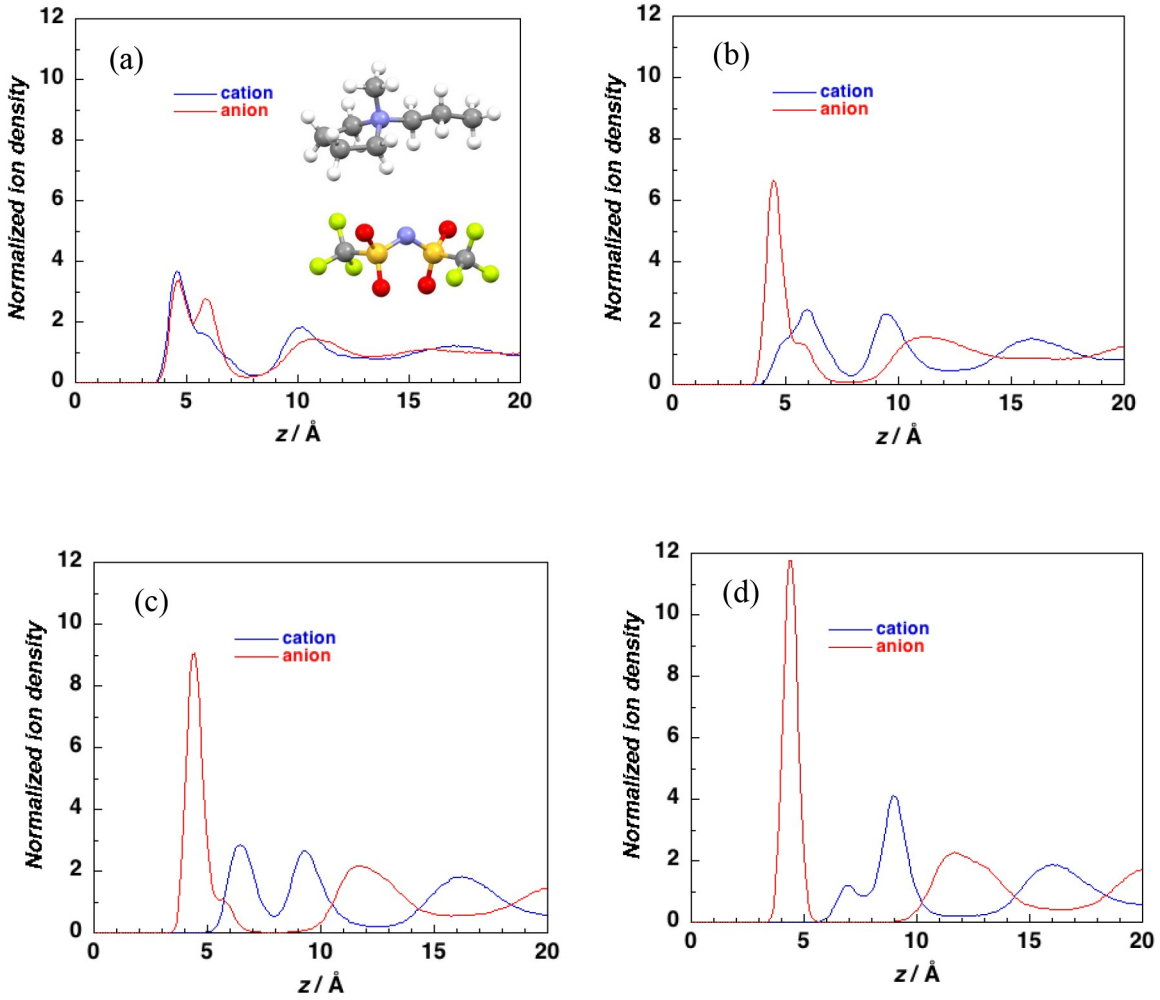

Figure 4. Normalized density of cation and anion near positively charged graphene obtained by MD simulations of [pmpyro][TFSA] ionic liquid. a) Carbon atoms of graphene have no charges; b) carbon atoms of graphene at $z=0$ Å have 0.01 e and those at $z=200$ Å have −0.01 e; c) carbon atoms of graphene at $z=0$ Å have 0.02 e and those at $z=200$ Å have −0.02 e; d) carbon atoms of graphene at $z=0$ Å have 0.03 e and those at $z=200$ Å have −0.03 e.

around 10 Å correspond to the ions which do not have contact with the graphene sheets as shown in Figure 5b and 5d.

The ion densities near positively charged graphene sheet depend strongly on the magnitude of charges on the graphene sheet. The normalized ion densities calculated for the [pmpyro][TFSA] ionic liquid near positively charged graphene sheet are shown in Figures 4b–d. The charges of carbon atoms of the graphene sheet ($z=0$ Å) in the MD simulations in Figure 4b, 4c and 4d are 0.01, 0.02 and 0.03 e, respectively. The comparison of Figures 4a and 4b shows that the density of anion at $z=4$ Å increases, while that at $z=6$ Å decreases when the charges on carbon atoms of the graphene change from 0.0 to 0.01 e. The density of cation at $z=4$ Å decreases and that at $z=6$ Å increases by the same change of the charges on carbon atoms of the graphene sheet. The changes of peak heights suggest that the population of ions in the two environments near the graphene sheet changes by the charges on the graphene. Figure 4c and 4d show that further increase of the positive charges on the graphene sheet increases the density of anion at $z=4$ Å, while the density of cation at $z=4$ Å decreases. The peak of the density of cation at $z=4$ Å disappears when the charges on carbon atoms of graphene increase up to 0.02 e. The peak of the density of cation at $z=6$ Å decreases by the increase of the charges on graphene, the peak still exists when the charges on carbon atoms of graphene increase up to 0.03 e, while the peak moves to $z=7$ Å. This peak of the density of cation suggests that a few cations still exists close to the graphene, even when each carbon atom of the graphene has positive charge (0.03 e). The peaks around $z=10$ Å are ions which do not have contact with the graphene. By the increase of the positive charge of the graphene, the peak of the density of cation around $z=10$ Å increases, while the peak of anion shifts from $z=10$ Å (Figure 4a) to $z=12$ Å (Figure 4d) to form the charge-ordering structure.

The normalized ion densities calculated for the [pmpyro][TFSA] ionic liquid near negatively charged graphene sheet are shown in Figure 6. The charges of carbon atoms of graphene sheet in the MD simulations in Figure 6a, 6b, 6c and 6d are 0.0, −0.01, −0.02 and −0.03 e, respectively. The comparison of the Figures 6a and 6b shows that the density of anion at $z=196$ Å

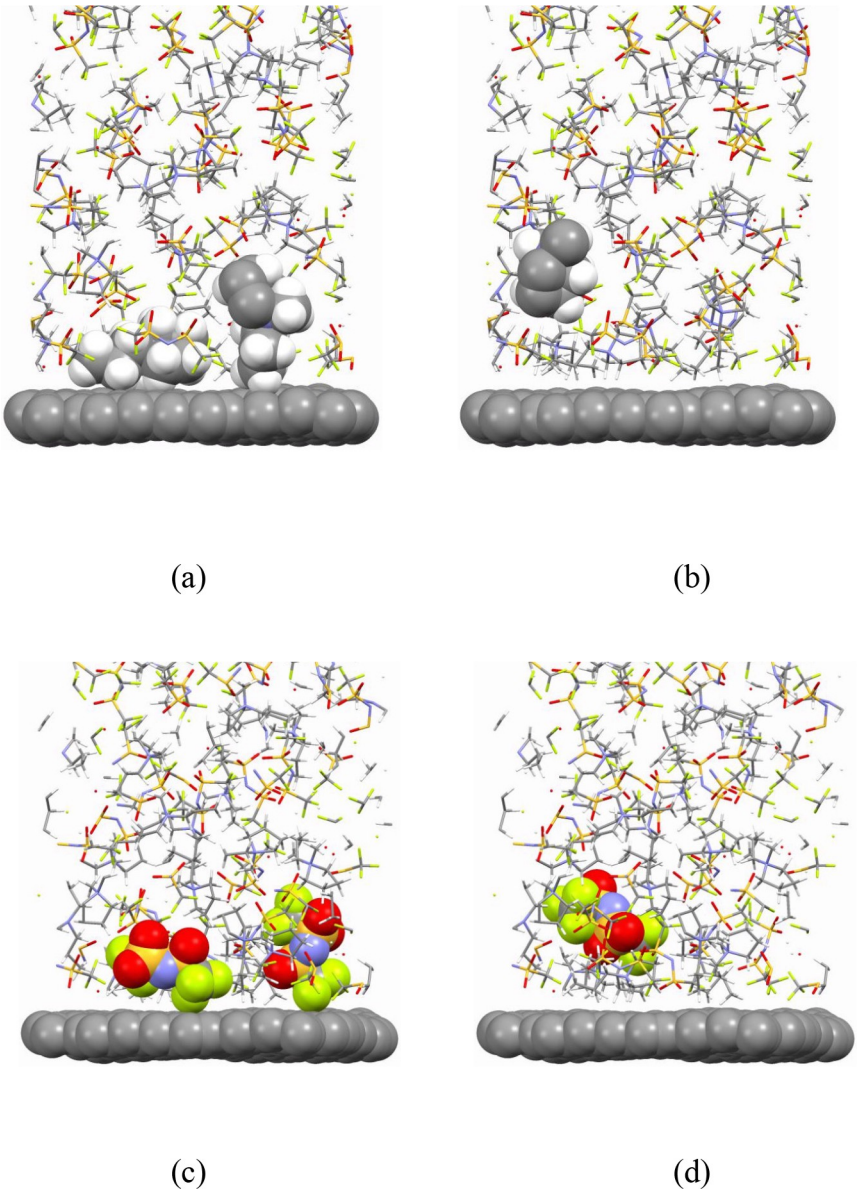

Figure 5. Cation and anion in [pmpyro][TFSA] ionic liquid near graphene. a) $[pmpyro]^+$ cations in $z=4$–7 Å; (b) $[pmpyro]^+$ cations in $z>10$ Å (c) $[TFSA]^-$ anions in $z=4$–7 Å; (d) $[TFSA]^-$ anions in $z>10$ Å.

(4 Å from the graphene sheet) decreases, while the density at $z=194$ Å (6 Å from the graphene sheet) increases when the charges of carbon atoms of graphene sheet at $z=200$ Å change from 0.0 to −0.01 e. The density of cation at $z=196$ Å increases and that at $z=194$ Å decreases by the increase of the negative charges of carbon atoms of graphene sheet. The increase of the cation density at $z=196$ Å suggests that the increase of cations which have contact with the graphene in parallel orientation to the graphene. However, the total distribution of the orientation of cations in the first layer ($z=194$–196 Å) is still unclear, since the orientation of cations at $z=194$ Å is uncertain. Further increase of the negative charges on the graphene sheet enhances the peak of cation at $z=196$ Å, while decreases the peak of anion at $z=194$ Å. By the increase of the negative charge on the graphene sheet, the peak of anion around $z=190$ Å is enhanced, while the peak of cation around $z=190$ Å moves around $z=186$ Å to form the charge-ordering structure.

The normalized ion densities hardly change with charge on graphene sheets in the region far enough from graphene sheets, in contrast to those near charged graphene sheets. The normalized ion densities at around 100 Å from graphene obtained by MD simulations are shown in Figure S1.

2.3. Ion Density of [pmpyro][FSA] Ionic Liquid near Charged Graphene

The charge-ordering structure produced in the [pmpyro][FSA] ionic liquid is significantly different from that produced in the

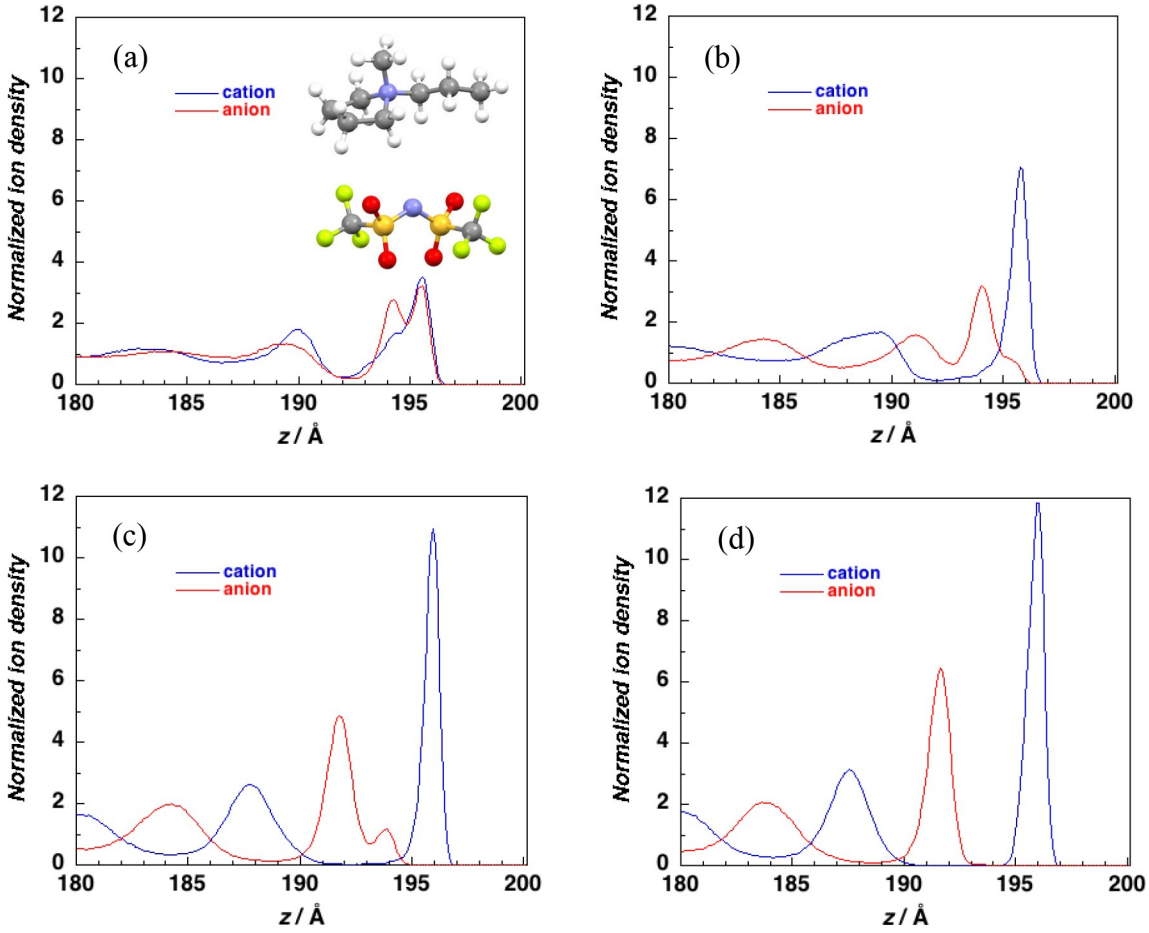

Figure 6. Normalized density of cation and anion near negatively charged graphene obtained by MD simulations of [pmpyro][TFSA] ionic liquid. a) Carbon atoms of graphene have no charges; b) carbon atoms of graphene at $z=0$ Å have 0.01 e and those at $z=200$ Å have −0.01 e; c) carbon atoms of graphene at $z=0$ Å have 0.02 e and those at $z=200$ Å have −0.02 e; d) carbon atoms of graphene at $z=0$ Å have 0.03 e and those at $z=200$ Å have −0.03 e.

[pmpyro][TFSA] ionic liquid. The normalized ion densities calculated for the [pmpyro][FSA] ionic liquid sandwiched by graphene sheets without charges is shown in Figure 7a. The calculated ion densities show that the [pmpyro][FSA] ionic liquid has structure in the range of 20 Å from graphene sheet as in the case of the [pmpyro][TFSA] ionic liquid. The carbon atoms of graphene at $z=0$ Å have 0.01 e and those at $z=200$ Å have −0.01 e in the MD simulation of Figure 7b. The charges of carbon atoms in the MD simulations in Figure 7c and 7d are ± 0.02 and ± 0.03 e, respectively. The [pmpyro][TFSA] ionic liquid has long-range charge-ordering structure, when the ionic liquid is sandwiched with charged graphene sheets. The charge-ordering structure is observed from graphene down to nearly 80 Å. The range of charge-ordering structure observed in the [pmpyro][FSA] ionic liquid is significantly longer than that in the [pmpyro][TFSA] ionic liquid. Figures 7b–7c shows that the decay of charge-ordering structure near negatively charged graphene sheet is slightly slower than that near positively charged graphene sheet.

The normalized ion densities calculated for the [pmpyro][FSA] ionic liquid near charged graphene sheets are different from those for the [pmpyro][TFSA] ionic liquid as shown in Figures S2 and S3 in supporting information. The density of anion has two peaks at $z=4$ and 6 Å as in the case of the [pmpyro][TFSA] ionic liquid when graphene sheet has no charges, which suggests that there exist anions under two different environments near the graphene sheets as in the case of the [pmpyro][TFSA] ionic liquid. On the other hand, the density of cation has only one peak at $z=5$ Å. The comparison of the ion densities of [pmpyro][TFSA] and [pmpyro][FSA] ionic liquids shows that the anion in the ionic liquid affects the distribution of cations near graphene sheets. Although the heights of first peaks of the normalized ion densities (nearest peaks from the graphene sheets) for the [pmpyro][FSA] ionic liquid, are not largely different from those for the [pmpyro][TFSA] ionic liquid, the heights of other (second, third, etc.) peaks in the [pmpyro][FSA] ionic liquid are higher than the corresponding peaks in the [pmpyro][TFSA] ionic liquid. The density of cations near the positively charged graphene sheet at $z=5$–9 Å and the density of anions near the negatively charged graphene sheet at $z=191$–194 Å have only single peak (the second peak from the graphene sheet), respectively, in the [pmpyro][FSA] ionic liquid when the carbon atoms of graphene sheets have ± 0.02 e. On the other hand, the ion

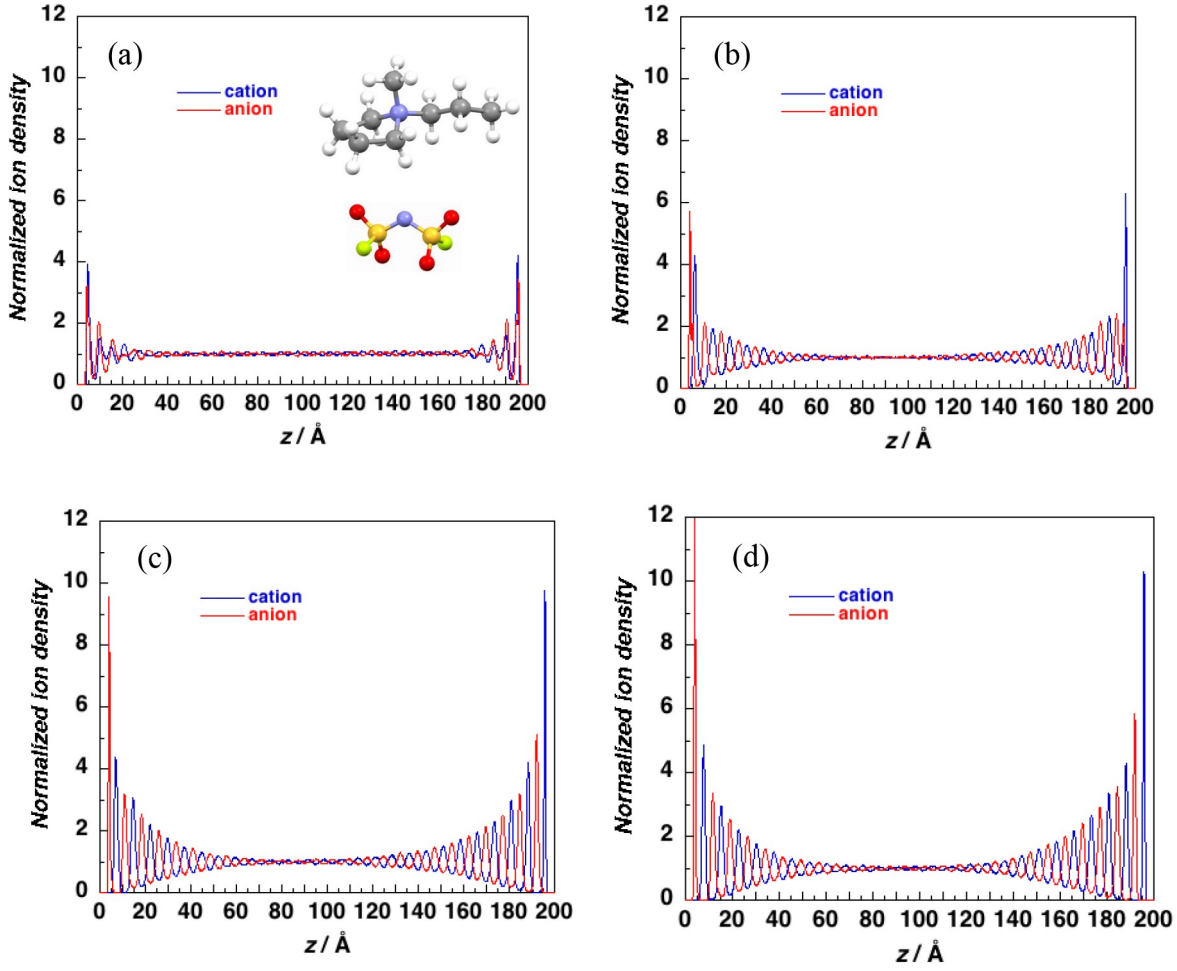

Figure 7. Normalized density of cation and anion obtained by MD simulations of [pmpyro][FSA] ionic liquid. a) Carbon atoms of graphene have no charges; b) carbon atoms of graphene at $z=0$ Å have 0.01 e and those at $z=200$ Å have −0.01 e; c) carbon atoms of graphene at $z=0$ Å have 0.02 e and those at $z=200$ Å have −0.02 e; d) carbon atoms of graphene at $z=0$ Å have 0.03 e and those at $z=200$ Å have −0.03 e.

densities in the [pmpyro][TFSA] ionic liquid have two peaks in the corresponding regions and heights of the normalized ion densities are lower compared with the [pmpyro][FSA] ionic liquid. The distance between neighboring peaks of the ion densities observed in the charge ordering structure of [pmpyro][FSA] ionic liquid is shorter than that observed in [pmpyro][TFSA] ionic liquid. The calculated ion densities show that the [pmpyro][FSA] ionic liquid has stronger charge-ordering structure near the charged graphene sheets compared with the [pmpyro][TFSA] ionic liquid. The smaller size of the $[FSA]^-$ anion compared with the $[TFSA]^-$ anion enhances the electrostatic interactions per volume, which will be one of the causes of the observed stronger charge-ordering structures. The stronger charge-ordering structure near the graphene sheets will be the cause of the longer charge-ordering structures observed in the [pmpyro][FSA] ionic liquid compared with the [pmpyro][TFSA] ionic liquid.

2.4. Anion Effects on Ion Density of [pmpyro]-Based Ionic Liquid

The charge-ordering structures of ionic liquids depend on anion strongly. The normalized ion densities calculated for the [pmpyro][CF_3SO_3], [pmpyro][CF_3CO_2], [pmpyro][PF_6] ionic liquids sandwiched by charged graphene sheets are shown in Figure 8a-c, respectively. The charges of carbon atoms in the MD simulations in Figure 8a-c are ± 0.02 e. The charge-ordering structures are observed in the [pmpyro][CF_3SO_3] and [pmpyro][CF_3CO_2] ionic liquids from graphene sheet down to nearly 60 Å as shown in Figures 8a and 8b. The range of charge-ordering structures observed in these ionic liquids is longer than that in the [pmpyro][TFSA] ionic liquid. The [pmpyro][PF_6] ionic liquid has very long charge-ordering structure, when the ionic liquid is sandwiched with charged graphene sheets, as shown in Figure 8c. The charge-ordering structure is observed from graphene sheet down to nearly 100 Å. The range of charge-ordering structures observed in the [pmpyro][PF_6] ionic liquids is longer than that in the [pmpyro][FSA] ionic liquid. Similar anion dependence of the range of charge-ordering structure

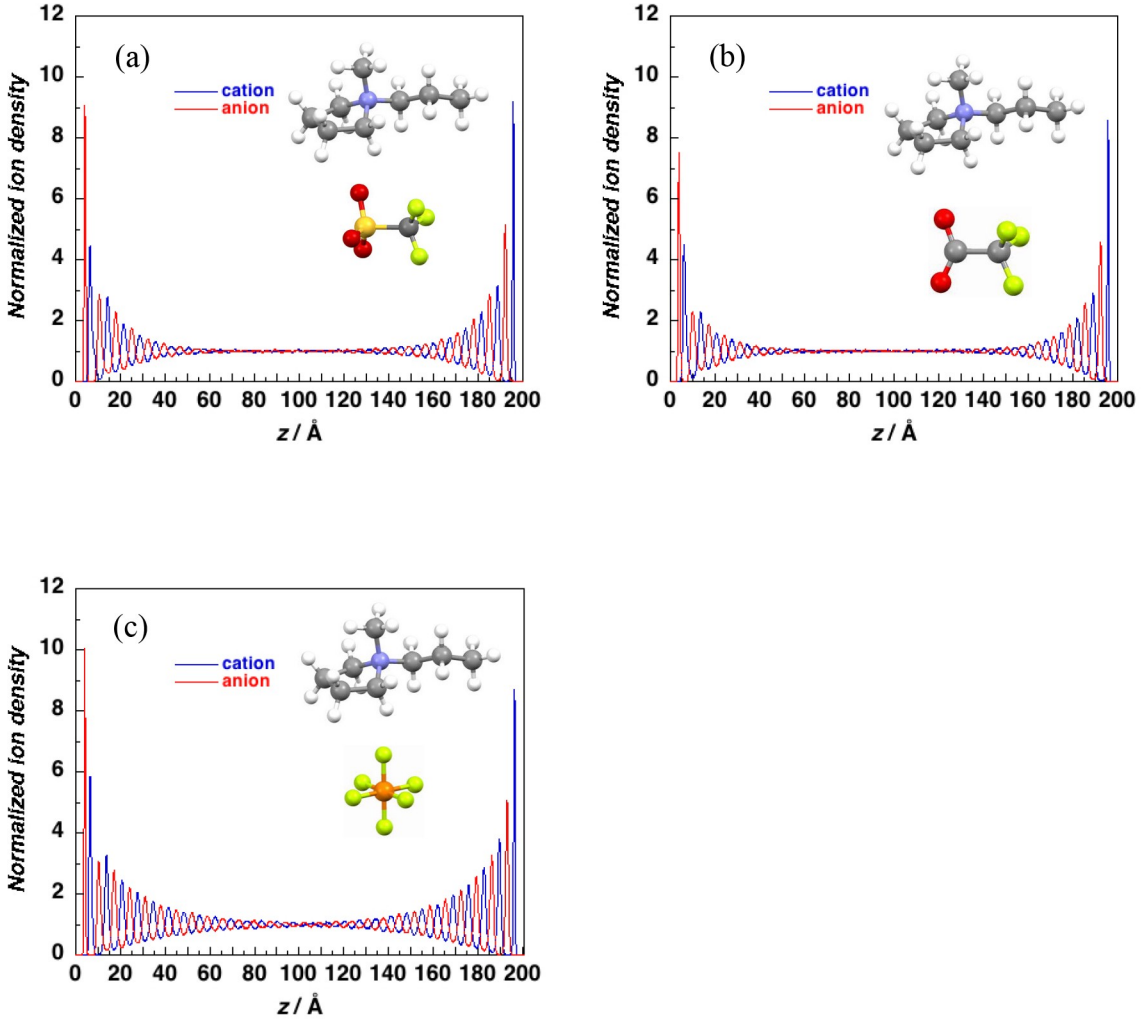

Figure 8. Normalized density of cation and anion obtained by MD simulations of ionic liquids. Carbon atoms of graphene at $z=0$ Å have 0.02 e and those at $z=200$ Å have −0.02 e, a) [pmpyro][CF_3SO_3]; b) [pmpyro][CF_3CO_2]; c) [pmpyro][PF_6].

was observed when the charges of carbon atoms in the graphene sheets are ±0.01 and ±0.03 e. Normalized ion densities in the [pmpyro][TFSA], [pmpyro][FSA], [pmpyro][CF_3SO_3], [pmpyro][CF_3CO_2] and [pmpyro][P_3F_6] ionic liquid when the charges of carbon atoms in the graphene sheets are ±0.01 e are shown in Figure 3b, 7b, S4b, S7b and S10b. Those when the charges of carbon atoms in the graphene sheets are ±0.03 e are shown in Figure 3d, 7d, S4d, S7d and S10d.

The ion densities in the [pmpyro][CF_3SO_3] ionic liquid near charged graphene sheets are substantially different from those in the [pmpyro][TFSA] and [pmpyro][FSA] ionic liquids. The ion densities in the [pmpyro][CF_3SO_3] ionic liquid is shown in Figures S4–S6. The density of the $CF_3SO_3^-$ anion has only one peak at $z=5$ Å when the graphene sheet has no charges, while the density of the anion has two peaks at $z=4$ and 5 Å, when the carbon atoms of graphene sheets have 0.01 e. The two peaks suggest that there exist $CF_3SO_3^-$ anions under two different environments near the graphene sheets as in the case of the [pmpyro][TFSA] ionic liquid. The density of anion further changes by the increase of positive charges on the graphene sheet. The density of anion has a peak at $z=4$ Å when the charges of carbon atoms of the graphene sheet is 0.02 or 0.03 e. The density of cation has two peaks at $z=4$ and 6 Å when the carbon atoms of graphene sheet have no charges, while the density of cation has a peak around $z=7$ Å when the carbon atoms of graphene have 0.01 e. The density of the cation has a shoulder peak at 8 Å when carbon atoms of graphene have 0.02 e or 0.03 e. The densities of ions in the [pmpyro][CF_3SO_3] ionic liquid near the negatively charged graphene sheet are similar to those observed in the [pmpyro][FSA] ionic liquid. The cation density has a peak at $z=196$ Å when the graphene sheet at $z=200$ Å has negative charges. The density of anion has two peaks at $z=192$ and 195 Å when the charges of carbon atoms of the graphene sheets are −0.01e, while the density of anion has one peak at $z=192$ Å when the charges are −0.02 or −0.03 e.

The ion densities in the [pmpyro][CF_3CO_2] ionic liquid near charged graphene sheets are slightly different from those in the [pmpyro] [CF_3SO_3] ionic liquid. The ion densities in the [pmpyro][CF_3CO_2] ionic liquid are shown in Figures S7–S9. The

density of $CF_3CO_2^-$ anion has only one peak at $z=4$ Å near the graphene sheets without charges and near the positively charged graphene sheet. The density of cation has two peaks at $z=4$ and 6 Å when the graphene sheet has no charges, while the density of cation has a peak around $z=7$ Å when the graphene sheet has positive charges as in the case of the [pmpyro][CF_3SO_3] ionic liquid. The density of cation has one peak at $z=196$ Å when the graphene sheet at $z=200$ Å has negative charges. The density of anion has two peaks at $z=192$ and 196 Å when the charges of carbon atoms of the graphene sheet are −0.01e, while the density of anion has one peak at $z=192$ Å when the charges are −0.02 or −0.03 e.

The ion densities in the [pmpyro][PF_6] ionic liquid near charged graphene sheets are similar to those observed in the [pmpyro][CF_3CO_2] ionic liquid. The effects of graphene charges on the ion densities of the [pmpyro][PF_6] ionic liquid are shown in Figures S10-S12. The density of the PF_6^- anion have only one peak at $z=4$ Å near the graphene sheets without charges and near the positively charged graphene sheet as in the case of the [pmpyro][CF_3CO_2] ionic liquid. The density of cation has two peaks at $z=4$ and 6 Å when the carbon atoms of graphene sheet has no charges, while the density of cation has a peak around $z=7$ Å when the graphene sheet has positive charges as in the case of the [pmpyro][CF_3SO_3] and [pmpyro][CF_3CO_2] ionic liquids. The ion densities near negatively charged graphene sheet are similar to those in the [pmpyro][CF_3SO_3] and [pmpyro][CF_3CO_2] ionic liquids. The cation density has one peak at $z=196$ Å when the graphene sheet at $z=200$ Å has negative charges. The density of anion has two peaks at $z=193$ and 196 Å when the charges of carbon atoms of the graphene sheet are −0.01e, while the density of anion has one peak at $z=193$ Å when the charges are −0.02 or −0.03 e. The [pmpyro][PF_6] ionic liquid has strong charge-ordering structure near the charged graphene sheets, probably owing to the small anion size. The strong charge-ordering structure near the graphene sheets will be the cause of the very long charge-ordering structures observed in the [pmpyro][PF_6] ionic liquid.

3. Conclusions

Molecular dynamics simulations of five $[pmpyro]^+$ cation-based ionic liquids sandwiched by charged graphene sheets show that the liquid structures of the ionic liquid depend strongly on the choice of anion. Long-range charge ordering structures were observed when the ionic liquids are sandwiched by charged graphene sheets. Although the magnitude of the oscillation of density of cation and anion near charged graphene sheets is enhanced by the increase of the charges on the graphene sheets, the range of the observed charge-ordering structures does not largely change. The range of charge-ordering structures depends strongly on the anion. The ranges change from 40 Å to 100 Å depending on the anion. The comparison of the charge-ordering structure observed in the [pmpyro][FSA] ionic liquid compared with that of the [pmpyro][TFSA] ionic liquid and the very long charge ordering structure in the [pmpyro][PF_6] ionic liquid suggest that the anion size plays important roles in determining the strength and range of the charge-ordering structures, although some other factors also affect the charge-ordering structures. The attraction by the electrostatic interactions in ionic liquids is enhanced by the decrease of the anion size, which will enhance the charge-ordering structure.

Acknowledgments

This work was supported by the ALCA program of Japan Science and Technology Agency (JST), MEXT program "Elements Strategy Initiative to Form Core Research Center" of the Ministry of Education, Culture, Sports, Science, and Technology (MEXT) of Japan, and JSPS KAKENHI Grant No. 18H03926 in parts.

Conflict of Interest

The authors declare no conflict of interest.

Keywords: Electrode · interface · ion density · ionic liquids · molecular dynamics

[1] M. Armand, F. Endres, D. R. MacFarlane, H. Ohno, B. Scrosati, *Nature Mat.* **2009**, *8*, 621–629.
[2] M. Galinski, A. Lewandowski, I. Stepniak, *Electrochimca Acta* **2006**, *51*, 5567–5580.
[3] C. Zhong, Y. Deng, W. Hu, J. Qiao, L. Zhang, J. Zhang, *Chem. Soc. Rev.* **2015**, *44*, 7484–7539.
[4] A. Noda, K. Hayamizu, M. Watanabe, *J. Phys. Chem. B* **2001**, 105, 4603.
[5] N. Nanbu, T. Kato, Y. Sasaki, F. Kitamura, *Electrochemistry* **2005**, *73*, 610–613.
[6] F. W. Richey, Y. A. Elabd, *J. Phys. Chem. Lett.* **2012**, *3*, 3297–3301.
[7] S. A. Kislenko, I. S. Samoylov, R. H. Amirov, *Phys. Chem. Chem. Phys.* **2009**, *11*, 5584–5590.
[8] K. Motobayashi, Y. Shibamura, K. Ikeda, *Electrochem. Commun.* **2019**, *100*, 117–120.
[9] S. Baldelli, *Acc. Chem. Res.* **2008**, *41*, 421–431.
[10] W. Zhou, S. Inoue, T. Iwahashi, K. Kanai, K. Seki, T. Miyamae, D. Kim, Y. Katayama, Y. Ouchi, *Electrochem. Commun.* **2010**, *12*, 672–675.
[11] B. Braunschweig, P. Mukherjee, J. L. Haan, D. D. Dlott, *J. Electroanaly. Chem.* **2017**, *800*, 144–150.
[12] R. Akin, N. Borisenko, M. Drushler, S. Z. El Abedin, F. Endres, R. Hayes, B. Huber, B. Roling, *Phys. Chem. Chem. Phys.* **2011**, *13*, 6849–6857.
[13] S. Ge, M. Yan, J. Lu, M. Zhang, F. Yu, J. Yu, X. Song, S. Yu, *Biosensors Bioelectronics* **2012**, *31*, 49–54.
[14] B. McLean, H. Li, R. Stefanovic, R. J. Wood, G. B. Webber, K. Ueno, M. Watanabe, G. G. Warr, A. Page, R. Atkin, *Phys. Chem. Chem. Phys.* **2015**, *17*, 325–333.
[15] R. Wen, B. Rahn, O. M. Magnussen, *Angew. Chem. Int. Ed.* **2015**, *54*, 6062–6066; *Angew. Chem.* **2015**, *127*, 6160–6164.
[16] A. Lahiri, G. Z. Li, M. Olschewski, F. Endres, *ACS Appl. Mat. Interface* **2016**, *8*, 34143–34150.
[17] L. A. Jurado, R. M. Espinosa-Marzal, *Sci. Rep.* **2017**, *7*, 4225.
[18] M. V. Fedorov, A. A. Maxim, *J. Phys. Chem. B* **2008**, *112*, 11868–11872.
[19] J. Vatamanu, O. Borodin, G. D. Smith, *J. Am. Chem. Soc.* **2010**, *132*, 14825–14833.
[20] C. Zhan, C. Lian, Y. Zhang, M. W. Thompson, Y. Xie, J. Wu, P. R. C. Kent, P. T. Cummings, D. Jiang, D. J. Wesolowski, *Adv. Sciecnece* **2017**, *4*, 1700059.
[21] M. Sha, G. Wu, Q. Dou, Z. Tang, H. Fang, *Langmuir* **2010**, *26*, 12667–12672.
[22] J. Vatamanu, O. Borodin, G. D. Smith, *J. Phys. Chem.* **2012**, *116*, 1114–1121.

[23] C. Merlet, B. Rotenberg, P. A. Madden, M. Salanne, *Phys. Chem. Chem. Phys.* **2013**, *15*, 15781–15792.
[24] A. Uysal, H. Zhou, G. Feng, S. S. Lee, S. Li, P. Fenter, P. T. Cummings, P. F. Fulvio, S. Dai, J. K. McDonough, Y. Gogotsi, *J. Phys. Chem. C* **2014**, *118*, 569–574.
[25] R. Futamura, T. Iiyama, Y. Takesaki, Y. Gogotsi, M. J. Biggs, M. Salanne, J. Segalini, P. Simon, K. Kaneko, *Nature Mat.* **2017**, *16*, 1225–1232.
[26] H. Yildirim, J. B. Haskins, C. W. Bauschlicher Jr., J. W. Lawson, *J. Phys. Chem. C* **2017**, *121*, 28214–2823.
[27] Y. Yokota, H. Miyamoto, A. Imanishi, K. Inagaki, Y. Morikawa, K. Fukui, *Phys. Chem. Chem. Phys.* **2018**, *20*, 6668–6676.
[28] Y. Zhang, B. Dyatkin, P. T. Cummings, *J. Phys. Chem. C* **2019**, *123*, 12583–12591.
[29] C. Noh, Y.-J. Jung, *Phys. Chem. Chem. Phys.* **2019**, *21*, 6790–6800.
[30] V. V. Chaban, N. A. Andreeva, E. Fileti, *New J. Chem.* **2018**, *42*, 18409–18417.
[31] J. B. Haskins, W. R. Bennett, J. J. Wu, D. M. Hernandez, O. Borodin, J. D. Monk, C. W. Bauschlicher, J. W. Lawson, *Phys. Chem. B* **2014**, *118*, 11295–11309.
[32] S. Begic, e. Jonsson, F. Chen, M. Forsyth, *Phys. Chem. Chem. Phys.* **2017**, *19*, 30010–30020.
[33] S. Sharma, H. K. Kashyap, *J. Phys. Chem. C* **2017**, *121*, 13202–13210.
[34] S. Sharma, H. S. Dhattarwal, H. K. Kashyap, *J. Mol. Liq.* **2019**, *291*, 111269.
[35] S. Plimpton, *J. Comp. Phys.* **1995**, *117*, 1–19.
[36] J. P. Ryckaert, G. Ciccotti, H. J. C. Berendsen *J. Comput. Phys.* **1997**, *23*, 327.
[37] G. J. Martyna, M. L. Klein, M. Tuckerman, *J. Chem. Phys.* **1992**, *97*, 2635.
[38] S. Tsuzuki, W. Shinoda, H. Saito, M. Mikami, H. Tokuda, M. Watanabe, *J. Phys. Chem. B* **2009**, *113*, 10641.

Manuscript received: December 1, 2019
Revised manuscript received: March 3, 2020
Accepted manuscript online: March 4, 2020
Version of record online: March 19, 2020